

## Article

# Feature Encoding and Selection for Iris Recognition Based on Variable Length Black Hole Optimization

Tara Othman Qadir Saraf <sup>1,2,\*</sup> , N. Fuad <sup>3</sup> and N. S. A. M. Taujuddin <sup>3</sup>

<sup>1</sup> Faculty of Computer Science and Information Technology, Universiti Tun Hussein Onn Malaysia (UTHM), Parit Raja 86400, Johor, Malaysia

<sup>2</sup> Faculty of Software and Informatics Engineering, College of Engineering, Salahaddin University, Erbil 44001, Kurduistan, Iraq

<sup>3</sup> Faculty of Electrical and Electronic Engineering, Universiti Tun Hussein Onn Malaysia (UTHM), Parit Raja 86400, Johor, Malaysia

\* Correspondence: alsaraftara@gmail.com; Tel.: +60-01137065258

**Abstract:** Iris recognition as a biometric identification method is one of the most reliable biometric human identification methods. It exploits the distinctive pattern of the iris area. Typically, several steps are performed for iris recognition, namely, pre-processing, segmentation, normalization, extraction, coding and classification. In this article, we present a novel algorithm for iris recognition that includes in addition to iris features extraction and coding the step of feature selection. Furthermore, it enables selecting a variable length of features for iris recognition by adapting our recent algorithm variable length black hole optimization (VLBHO). It is the first variable length feature selection for iris recognition. Our proposed algorithm enables segments-based decomposition of features according to their relevance which makes the optimization more efficient in terms of both memory and computation and more promising in terms of convergence. For classification, the article uses the famous support vector machine (SVM) and the Logistic model. The proposed algorithm has been evaluated based on two iris datasets, namely, IITD and CASIA. The finding is that optimizing feature encoding and selection based on VLBHO is superior to the benchmarks with an improvement percentage of 0.21%.

**Keywords:** black hole optimization; feature encoding; feature selection; high dimensionality; iris recognition; variable length optimization



**Citation:** Saraf, T.O.Q.; Fuad, N.; Taujuddin, N.S.A.M. Feature Encoding and Selection for Iris Recognition Based on Variable Length Black Hole Optimization. *Computers* **2022**, *11*, 140. <https://doi.org/10.3390/computers11090140>

Academic Editors: Phivos Mylonas, Katia Lida Kermanidis and Manolis Maragoudakis

Received: 26 June 2022

Accepted: 3 September 2022

Published: 16 September 2022

**Publisher's Note:** MDPI stays neutral with regard to jurisdictional claims in published maps and institutional affiliations.



**Copyright:** © 2022 by the authors. Licensee MDPI, Basel, Switzerland. This article is an open access article distributed under the terms and conditions of the Creative Commons Attribution (CC BY) license (<https://creativecommons.org/licenses/by/4.0/>).

## 1. Introduction

Advances in computer technologies and biometrics are having a huge impact on security applications for society [1]. Human identification using biometric technologies has attracted more attention in security applications. Some examples of security applications are access control [2], border control, [3], banking [4], and forensics [5]. Human recognition research projects promise new life to many security-consulting firms and personal identification system manufacturers. There are various biometric technologies such as iris [6], face [7], fingerprint [8], palm print [9], hand geometry [10], voice [11] and veins [12]. Among these technologies, iris recognition has received more attention due to its inconvenient usage as security for various systems [13].

Following the fundamental principle that interclass variation should be larger than intraclass variation, iris patterns offer a powerful alternative approach to reliable visual recognition of persons when imaging can be done at distances of about a meter or less, and especially when there is a need to search very large databases without incurring any false matches despite a huge number of possibilities. Although it is small with an 11 mm diameter and sometimes problematic to image, the iris has the great mathematical advantage that its pattern variability among different persons is enormous. In addition, as an internal organ of the eye, the iris is well protected from the environment and stable

over time. Iris is robust to ageing factors compared with other biometrics authentication parts of the human. As a planar object, its image is relatively insensitive to the angle of illumination, and changes in viewing angle cause only affine transformations; even the nonaffine pattern distortion caused by pupillary dilation is readily reversible in the image coding stage [14].

Iris is regarded as one of the most trustworthy biometric traits for human identification for a variety of reasons, including the fact that it is a highly protected internal organ that is visible from the outside, and that iris patterns are highly distinctive with a high degree of freedom, that iris patterns are largely stable over time, etc. Modern iris recognition algorithms have shown encouraging results for iris recognition. Binary characteristics are used by the majority of iris recognition algorithms (i.e., iris codes). Iris recognition systems may be deployed widely because of the enormous advantages in memory and processing cost provided by the binary character of iris codes. With millions of individuals registered, the current countrywide iris recognition system deployments in the United Arab Emirates (UAE) [15] and India [16] are regarded as successful.

By quantifying the probabilistic information that random variables might potentially send to one another, information theory [17] examines correlations between them. Its techniques are appropriate for inference, communication channels, classifiers, and pattern recognition in general, but have not seen much use in the realm of biometrics outside of cryptographic protocols. This is strange because several ideas in biometrics, like the capacity of a noisy channel, an encoding scheme's efficiency, and the entropy of a random variable or code, strongly resemble these concepts. For instance, it is generally understood that the randomness and complexity of biometric patterns determine their individuality and, consequently, their capacity to avoid collisions with other individuals (False Matches), but these biometric properties are infrequently quantified in terms of entropy. It's time to develop a quantitative and comprehensive understanding of the genesis of biometric collision avoidance, especially now that roughly a billion people have had their iris codes registered in a national ID deployment across India for de-duplication checks [18].

Meta-heuristic searching optimization is a random searching algorithm with the capability of embedding heuristic knowledge for finding the best solution from a huge number of candidate solutions. Meta-heuristic searching algorithms are categorized under several categories such as discrete vs. continuous [19], single objective versus multi-objective [20], fixed length versus variable length [21], and evolutionary versus swarm [22]. One appealing application of meta-heuristic algorithms is the field of feature selections which aims at obtaining the best candidate number of features out of high possible selections and combinations. Considering that iris coding is a type of feature selection and recoding, using meta-heuristic searching optimization for this application has a high potential in increasing the performance in terms of recognition, noise filtering, memory reduction and computational efficiency. A limitation of the previously developed meta-heuristic algorithms is their assumption of fixed length or number of features. This is because the knowledge of the true number of relevant features is not available for all datasets

This article includes several contributions, they can be stated as follows

1. To the best of our knowledge, it is the first article that presents the problem of iris recognition from a feature selection perspective. Mainly, it presents a variable length of the number of features to be selected for optimizing the iris recognition performance instead of traditional methods that use a fixed-length number of features. This provides two benefits, namely, reducing the size of feature space needed for training and prediction which means memory reduction, and improving the accuracy considering the non-relevant features are removed.
2. It uses existing variable length black hole optimization for the purpose of feature selection in the context of iris recognition. This algorithm is selected due to the competing performance it provides compared with other similar methods such as variable length particle swarm optimization VLPSO [21].

- It compares the performance of variable length black hole optimization for feature selection in iris recognition using two feature spaces, namely, Gabor and LBP and using two classifiers, namely, support vector machine SVM and logistic regression model which shows the superiority of VLBHO over VLPSO.

The goal of this article is to adapt recently developed work by us in the field of iris coding and feature selection. Particularly, we use variable length black hole optimization for coding and selecting the best features in order to obtain reduced and relevant feature space. The remaining of the article is organized as follows. In Section 2, we present the background of iris coding. Next, the literature survey is given in Section 3. Afterwards, the methodology is presented in Section 4. Next, the experimental works and evaluation are given in Section 5. Lastly, the summary and conclusion are presented in Section 6.

## 2. Background of the Iris Coding

The background of the article consists of three sub-sections. In Section 2.1, we present the Gabor filter for feature extraction. Next, the Local Binary Pattern (LBP) is given in Section 2.2. Lastly, we present iris coding in Section 2.3.

### 2.1. Gabor

In recent years, computer vision has made extensive use of Gabor filter [18] based techniques, particularly for texture analysis. Elementary Gabor functions are sinusoidally modulated Gaussians. It is shown that the functional form of Gabor filters conforms closely to the receptive profiles of simple cortical cells, and Gabor filtering is an effective scheme for image representation. The representation of 2D Gabor can be given using the Equations (1)–(3)

$$G(x, y; \theta, f) = \exp\left\{-\frac{1}{2}\left[\frac{x'^2}{\delta_{x'}^2} + \frac{y'^2}{\delta_{y'}^2}\right]\right\} \cos(2\pi fx) \quad (1)$$

$$x' = x \cos \theta + y \sin \theta \quad (2)$$

$$y' = y \cos \theta - x \sin \theta \quad (3)$$

where

$f$  denotes the frequency of the sinusoidal plane wave along the direction  $\theta$  from  $x$ -axis, and it be chosen to be of power 2 such as 2, 4, 8, 16 and 32 cycles/degree

$\delta_{x'}$ ,  $\delta_{y'}$  are the space constants of the Gaussian envelop  $x'$ ,  $y'$  respectively

$\theta$  denotes the direction and it takes one of the values  $\theta = 0^\circ, 45^\circ, 90^\circ$  and  $135^\circ$

Each value of the parameters when it changed, it results in a different value of the Gabor

Having five values of the frequency and four values of the direction, we obtain 20 filter with the same size.

In addition to the original filtered images, we apply the mean and variance using Equation (4)

$$V = \frac{1}{N} \left( \sum_N |f(x, y) - m| \right) \quad (4)$$

$$\sigma_V = \sqrt{\frac{(\sum_N |f(x, y) - m|^2)}{N - 1}} \quad (5)$$

$m$  denotes the mean values of the filters

$N$  denotes the number of filters

### 2.2. Local Binary Pattern

Local binary pattern (LBP) [23] is an invariant measure for texture with grayscale format. The basic LBP works based on using  $3 \times 3$  neighbourhood of each pixel. The mask

is used to generate a binary pattern based on comparing each of the surrounding pixels with the central one based on the Equation (6)

$$f(I(z_0), I(z_i)) = \begin{cases} 1, & \text{if } I(z_i) - I(z_0) > \text{threshold} \\ 0, & \text{if } I(z_i) - I(z_0) \leq \text{threshold} \end{cases} \tag{6}$$

where

$i = 1, \dots, 8$  denotes the index of the surrounding pixels

$z_0$  indicates to the central pixel

The general representation of LBP with respect to radius  $R$  and neighbour  $P$  is given as in Equation (7)

$$LBP_{P,R} = \sum_{p=0}^{P-1} s(g_p - g_c)2^p \tag{7}$$

where

$$s(x) = \begin{cases} 1, & x \geq 0 \\ 0, & x < 0 \end{cases}$$

$g_p$  denotes the grayscale of the pixel

$g_c$  denotes the grayscale of the centre

### 2.3. Iris Coding

Assuming that we have  $f = [f_1 f_2 \dots f_n]^T \in \mathbb{R}^n$  is a vector of all feature's values extracted from an unwrapped iris image. Also, assuming that  $b = [b_1, b_2, \dots, b_n]^T$  is a binary vector of the iris code corresponding to  $f$  with  $n$  bits. For the  $i^{th}$  bit  $b_i$ , it is found based on the optimization and it presented in Table 1.

**Table 1.** The optimization formulas that are used for solving the iris coding [24].

Solution Pace	Formula 1	Formula 2	Formula 3	Formula 4
$b \in \{-1, 1\}^n$	$\ b - f\ _2^2$	$\sum_i (-f_i)b_i + \alpha \sum_i \sum_{j \in N^i}  b_i - b_j $	$-\sum_i f_i b_i + \beta \sum_i \sum_{j \neq i} b_i b_j$	$\sum_i (-f_i)b_i + \alpha \sum_i \sum_{j \in N^i}  b_i - b_j  + \beta \sum_i \sum_{j \neq i} b_i b_j$
Role	Binary coding of features values	Exploiting the vertical neighbour adjacency of the iris codes	Enhancing the stability or reduce bits flops	Jointly Exploiting the vertical neighbour adjacency and Enhancing the stability

The solving of this optimization problem can be performed by using iterative algorithm. The iterative algorithm starts by initializing  $b^0$  which denotes the initial binarizing and iteratively updating its value until convergence.

### 3. Literature Survey

The literature survey is decomposed into three sub-sections. The first sub-section is dedicated to present the literature of iris features extraction and it given in Section 3.1. The second one is the iris coding and it is presented in Section 3.2. The third one is the iris classification which is presented in Section 3.3.

#### 3.1. Feature Extraction

Several models are used to extract iris characteristics. The Gabor filter plays a crucial role in the depiction of iris texture because it delivers the best trade-off between spatial and frequency resolution. Iris texture will be divided into frequency over a range of sizes and orientations using gabor filtering. A survey of the literature reveals that different values of the filter parameters are utilized with Gabor filters, leading to different impacts on texture classification. Extremely dissimilar options emerged in the literature when researchers worked to find Gabor parameters in Gabor functions, suggesting that there is no standard

arrangement of Gabor filters for various texture representations. Ref. [25], state that Gabor filters with the right settings can significantly increase recognition rates because their filter banks may produce higher coverage in the Fourier domain, enabling the extraction of more discriminative information. Because of this, it might be challenging to determine the ideal Gabor filters for iris imaging from a range of acquisition situations, user groups, and devices. However, a thorough search of all viable parameters might not be feasible since Gabor parameter selection is a nonlinear, constrained programming problem with a number of continuous and discrete variables. The time-frequency transition makes it challenging to create a mathematical goal function between the performance of iris recognition using Gabor kernels. An iris data-driven Gabor filter optimization method is presented in [25], and is based on particle swarm optimization (PSO) and its binary version binary particle swarm optimization (BPSO). The latter are intended to find appropriate Gabor kernels and prevent the unreasoning predefinition of the Gabor filter. To build a set of data-driven Gabor kernels for fitting the most informative filtering bands, they used the particle swarm optimization technique and its binary counterpart. Next, they trained a deep belief network to capture complicated patterns from the ideal Gabor filtered coefficients.

The feature extraction step, which has the greatest impact on recognition performance, has recently been the subject of a lot of research investigations. Iris analysis in a certain transform domain using a specified type of filter is the most often used and well-studied approach among the several feature extraction methods. These techniques have the ability to identify texture characteristics that are absent in the spatial domain and to avoid noise in spatial iris pictures. However, they must all consider choosing appropriate filterers and transform kernels. In other studies, the idea was to describe iris texture information using geometric descriptors. They could simply and naturally design in the spatial realm. The performance of this type of approach is, however, rather prone to iris image noises. Combining several iris feature types is now thought to be a potential strategy. They might make up for the unimodal iris feature's shortcomings, but doing so would incur computing complexity and time costs. In Table 2, we provide overview of previous approaches for feature extraction in iris recognition.

**Table 2.** Overview of previous approaches for feature extraction in iris recognition.

Article	Category	Approach	Strength	Limitations
[26]	Filter based	Gabor, 2D Haar Wavelet Transform	Good immunity to illumination	The size of features is long
[27]	Filter based	quadrature 2-D Gabor wavelet coefficients with most-significant bits	Good immunity to illumination	Information loss
[28]	Filter based	wavelet transform (WT) zero crossings	Good discriminative performance	Requires feature selection

### 3.2. Feature Selection and Iris Coding

The following operational modules should fundamentally be included in an iris recognition system: picture capture, iris segmentation, normalization, feature extraction, matching, and recognition [29]. The two modules that directly affect the overall system accuracy out of these four are iris segmentation and feature extraction. As a result, these modules alone are the subject of the majority of the linked study. Feature selection blocks have only been added by a few numbers of researchers to the modules for iris recognition. A novel optimization approach of linked feature selection for cross-sensor iris identification was put out in the work of [30], The first portion of our model's objective function seeks to reduce misclassification errors, while the second part uses  $l_{2,1}$ -norm regularization to achieve sparsity in linked feature spaces. The suggested feature selection model may be thought of as a half-quadratic optimization problem during the training phase, with

an iterative algorithm being constructed to find the answer. An automated method for iris recognition based on 2-D iris photographs was created in the work of [31]. In order to reduce the dimensionality of iris characteristics without losing important information, the 2DPCA (two-dimensional principal component analysis) and GA (Genetic Algorithm) have been utilized as feature extraction and feature selection approaches. Levenberg-learning Marquardt's rule is used to create the Back Propagation Neural Network (BPNN) for iris recognition. In order to choose the best sub-component set, an iris recognition algorithm was presented in the work of [32], in the context of teaching learning-based optimization. It has been used to combine significant findings from the selection of several components. The Chebyshev distance classifier is used to relocate the optimal subsets. A filter-based approach to multiple feature construction using genetic programming (GP) called multiple feature construction (FCM) that stores the top individuals was proposed in the work of [33], and a filter-based approach to feature selection using GP named FS that employs a correlation-based evaluation method is also used. It is suggested to use a hybrid strategy called FCMFS, which first creates many features using FCM before choosing useful features using FS. The iris code was determined in the work of [24], from an optimization standpoint. Following their proof that the conventional iris code is the result of an optimization problem that reduces the distance between the feature values and the iris codes, they go on to show that more efficient iris codes can be produced by including terms in the objective function of this optimization problem. They also look into two more objective terms. The first objective term takes use of how an iris code's bits are arranged spatially in various places. The second target term reduces the impact of iris codes' less trustworthy bits. The two goal terms may be used separately or jointly to solve the optimization issue.

### 3.3. Iris Classification

The literature contains numerous articles with different type of classifiers used for iris classification. Three categories of application for iris recognition are found in the literature. The first one is iris recognition. In [34], iris segmentation, quality enhancement, and match score fusion for recognition were proposed. For segmenting the nonideal iris image, curve evolution approach is used based on modified Mumford-Shah functional. Furthermore, the algorithm uses enhancement algorithms applied on the iris image. For classification, support-vector-machine based learning algorithm for classification is used. The second category is for contact lens detection for improving iris recognition. A deep convolutional network with extensive connections between its layers, the Densely Connected Contact Lens Detection Network (DCLNet), has been suggested in [35]. Using support vector machines in addition to Densenet121, DCLNet was created through a number of modifications. The work of [36] has concentrated on a contact lens detection for improving iris recognition. Deep Convolutional Neural Network is utilized (CNN). The fifteen-layer CNN architecture ContlensNet is constructed for the three-class detection issue with the following classes: photographs with textured (or colorful), soft (or clear), and no contact lenses. The third category is fake iris detection. In ref. [37], fake iris detection algorithm is proposed based on improved local binary pattern and statistical features. It is combined of several steps. First, a simplified scale invariant feature detection descriptor is used for feature extraction at each pixel of the image. Second, scale invariant frequency transformation (SIFT) descriptor is used to rank the LBP encoding sequence. Next, statistical features are extracted from the weighted LBP map. Lastly, support vector machine is used for classification which has the role of classifying genuine and counterfeit iris images. In ref. [38], the effect of contact lenses on iris recognition has been studied. They have prepared iris contact lens databases: IIIT-Delhi Contact Lens Iris database and ND Contact Lens Detection 2013 database. In their work, they are interested in feature coding for the first category. In ref. [39], deep convolutional neural network is used for extracting features from iris. The approach uses an optimized center loss function to improve the insufficient discrimination caused by the traditional softmax loss function. For classification, cosine similarity is used to estimate the similarity between the features. In ref. [40], they have evaluated convolutional neural

networks (CNNs) on iris recognition. It has shown off-the-shelf CNN features for iris recognition. In order to extract features from the normalized iris pictures, five cutting-edge and commercial CNNs (AlexNet, VGG, Google Inception, ResNet, and DenseNet) are employed in this study. Each CNN has a number of levels, as you can see. The classification module is then given the recovered CNN feature vector. The Support Vector Machine (SVM) with many classes is then employed for classification. The iris classification problem is solved in ref. [41], using a multiclassification strategy based on the Hadamard error correction output code and a convolutional neural network. Following the fully connected layer and all convolutional layers for classification, the ReLU activation function is employed.

Overall, we observe that despite the significant amount of work that has been carried out in the scope of iris recognition. Less amount of work was performed in the role of feature selection for improving the performance of iris recognition in terms of memory and accuracy. Furthermore, the lacking of initial knowledge of the relevant number of features for iris recognition urges us to use variable length nature of algorithm for searching and optimizing the feature selection. Hence, the role of this article is to fill this research gap.

#### 4. Methodology

##### 4.1. Pre-Processing

The goal of pre-processing is to enhance the contrast in the image and to apply denoising operators. For this purpose, we use thresholding to isolate the image foreground from the background. Furthermore, contrast enhancement is used for improving the iris appearance in the data.

##### 4.2. Segmentation

The first step in iris identification is identifying the real iris area in a digital eye picture. The iris area is seen in Figure 1 and can be represented by two concentric circles: one for the iris/sclera border and the other for the iris/pupil boundary. In most cases, the eyelids and eyelashes cover the top and lower portions of the iris area. The iris area might experience specular reflections as well, which will alter the iris pattern. An approach is required to locate the circular iris region, separate and exclude these artefacts, and separate the circular iris region.

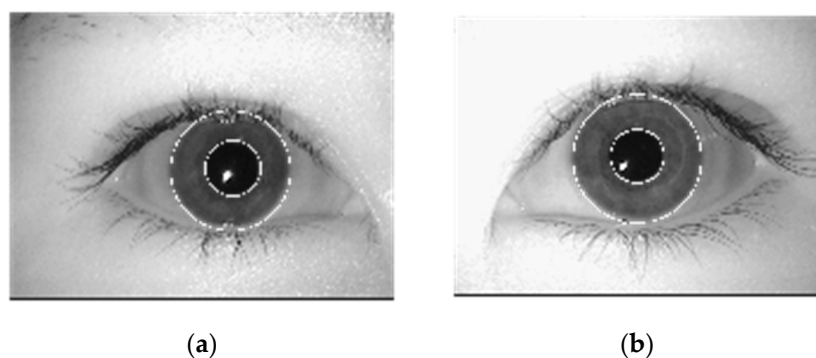


**Figure 1.** The results of the segmentation for samples taken from MMU dataset: (a) Left eye; (b) right eye.

The first derivatives of intensity values in an eye image are calculated, and then the result is thresholded to create an edge map. For edge detection, canny model is used. Votes are cast in Hough space for the parameters of circles travelling through each edge point based on the edge map. These are the  $x_c$  and  $y_c$  centre coordinates, as well as the radius  $r$ , which may be used to define any circle using the Equation (8).

$$x_c^2 + y_c^2 - r^2 = 0 \quad (8)$$

The eyelids can be detected using the parabolic Hough transform, which approximates the upper and lower eyelids with parabolic arcs, which are represented as;

$$-(x - h_j) \sin \theta_j + (y - k_j) \cos \theta_j)^2 = a_j((x - h_j) \cos \theta_j + (y - k_j) \sin \theta_j) \tag{9}$$

$a_j$  a parameter to control the curvature  
 $(h_j, k_j)$  to control the peak of the parabolic  
 $\theta_j$  denotes the angle of rotation relative to  $x$ -axis

For finding the circular iris and pupil regions, as well as the arcs of the upper and lower eyelids, it is also possible to use integro-differential operator employed by Daugman

$$\max_{(r, x_p, y_0)} \left| G_\sigma(r) * \frac{\partial}{\partial r} \oint_{r, x_0, y_0} \frac{I(x, y)}{2\pi r} ds \right| \tag{10}$$

$I(x, y)$  denotes the eye image  
 $r$  denotes the radius to search for  
 $G_\sigma(r)$  denotes gaussian smoothing function  
 $s$  denotes the contour of the circle given by  $r, x_0, y_0$

### 4.3. Iris Normalization

The division of the circular region produced using Daugman’s Model forms the foundation of the utilized enhanced normalizing technique. The approach divides the 360° region into a trapezoidal portion as shown in Figure 2.

1. Considering the lower half iris
2. Consider only percentage of the lower half circle
3. Now take the trapezoid form and change it to a rectangle by taking away the triangle shapes from both of its sides.
4. Acquire a tiny, rectangular, normalized picture of the iris for which the characteristics have been computed.

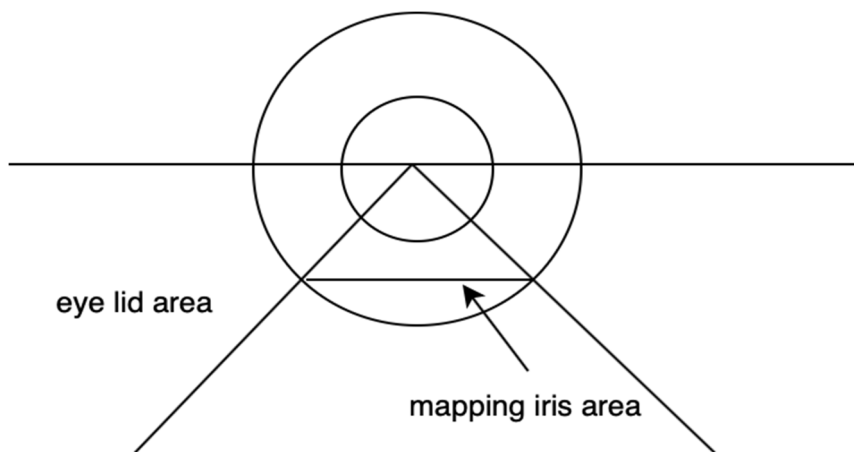


**Figure 2.** Geometric representation of iris normalization based on trapezoidal portion.

### 4.4. Feature Extraction

The iris has a particularly interesting structure and provides features information that are subject to ignorance. Hence, it is advised to explore representation methods that can describe both global and local information. In our representation, we aim at obtaining both global and local information from the iris. In our scheme, we map the iris image into a rectangular image that is divided into four sub-images and then we analyze the four sub-images. The combined vector of features contains the feature information that are extracted from each of the four sub-images. The extracted features from the sub-image are local descriptor that can still encode the global structure of the iris. Each of the extracted



features, contains the local information while the ordered sequence captures the invariant global representation.

#### 4.5. Feature Selection and Coding

For feature selection, we use variable length black hole optimization which is an extension to the common black hole optimization that was presented in [42]. In the original black hole optimization, the solutions imitate in its representation the state of the arts, their interaction with themselves or with a black hole and their mobility in the universe. In the original black hole, the algorithm was applied for clustering. In our recent work), an updated version of this algorithm has been proposed in order to make the algorithm capable of searching with variable length solution space which makes it suitable for feature selection. In addition, the algorithm proposed a new concept of energy to the black hole to replace it when it is no longer effective. Besides, it enables length changing of the solutions based on stagnation criterion. The algorithm adopts transfer function in order to enable searching within binary solution space. Two types of transfer functions are used: the first one is V-shape and the second one is S-shape. In this article, we use this algorithm for selecting the discriminative parts of the Gabor and LBP features. However, considering that the solution space is big, we will make the selection decision not for only single element of the feature vector but for single segment of the feature. In addition, we decide for changing the features from its original value to binary value based on the objective functions presented in Table 3. In this case, the solution vector will have two metameric variables: the first the metameric variable that is responsible of selecting certain segment of the two types of feature vectors and the second one is the metameric variable that is responsible of threshold the selected segment in order to optimize the mentioned objective function. In order to show the operation of the algorithm of feature selection and coding, we present the pseudo-code in Algorithm 1. As it is shown in the pseudocode, the algorithm takes a training dataset as input  $D$ , the segment size that is used for decomposing the feature vector before coding and selection, and the objective function formula. The output of the algorithm is the extracted features from the image. The algorithm performs a loop on the dataset images, and for each image it performs the operations of pre-processing, localizing, denoising, segmentation, feature extraction and concatenation of extracted features. Afterwards, the algorithm enables segmenting (or dividing) the feature vector into small segments using the parameter named segment size ( $SS$ ). Next, the algorithm call VLBHO for the goal of both selecting the relevant segments and binarizing them. The returned values from VLBHO is provided to obtain the extracted features  $F$ .

**Table 3.** Overview of optimization approaches for feature selection in iris recognition.

Article	Feature Selection	Optimization	Dataset
[30]	Coupled feature selection	Objective function of misclassification errors and norm regularization	CASIA
[31]	GA (Genetic Algorithm)	Reducing the dimensionality of the feature space	
[32]	Teaching learning based optimization	Similarity between sub-component	CASIA
[33]	Genetic programming	correlation-based evaluation two objective terms. The first objective term exploits the spatial relationships of the bits in different positions of an iris code. The second objective term mitigates the influence of less reliable bits in iris codes.	Freebase and YAGO
[24]	Solving objective function equation by using numerical approach		CASIAT ND0405 CASIAD UBIRS2

**Algorithm 1.** Pseudocode of features extraction and coding using VLBHO.**Input**

D // combined of set of labelled image with an iris part s for the purpose of training

SS // segment size

OF // objective function

**Output**

F // extracted features from the image

**Start Algorithm****For** each image in D

ProcessedImage = pre-processing (image)

IrisRegion = localization(ProcessedImage)

IrisRegion = denoising (IrisRegion)

Iris = Segmentation(IrisRegion)

[Gabor, LBP] = Extract(Iris)

Features = Concatenate(Gabor, LBP)

**End**

[smallSegments] = Segment(Gabor, LBP, SS)

Call VLBHO using OF

Return best solution that contains the coding threshold and the selected features

**End Algorithm**

#### 4.6. Classification

For classification, two models are used. The first one is the support vector machine (SVM) and the second is logistic regression classifier. We present each of them in the following sub-sections.

##### 4.6.1. Logistic Regression

This model uses regression fitting for classification the points. Logistic regression model calculates the class membership probability for one of the two categories in the data

$$P(1 | x, a) = \frac{1}{1 + e^{-(a \cdot x)}} \quad (11)$$

where

$a$  represents the hyper parameters

$x$  denotes the data

##### 4.6.2. Support Vector Machine

This classifier was based on the concept of hyper-plane decomposition for separating the data. However, it was developed further to solve non-linear problem by incorporation of Kernel. SVM uses several types of Kernels.

Polynomial homogenous type  $k(x, x') = (x \cdot x')^d$

Polynomial heterogenous type  $k(x, x') = (x \cdot x' + 1)^d$

Radial basis function  $k(x, x') = \exp(-\gamma \|x - x'\|^2)$ , for  $\gamma > 0$

Gaussian radial basis function  $k(x, x') = \exp(-\frac{\|x - x'\|^2}{2\sigma^2})$

#### 4.7. Datasets

This section provides the datasets that will be used for evaluation.

##### 4.7.1. CASIA.v4 Thousand

An expansion of CASIA-IrisV3, CASIA-IrisV4 has six subsets. The three CASIA-IrisV3 subsets are, respectively, CASIA-Iris-Interval, CASIA-Iris-Lamp, and CASIA-Iris-Twins. CASIA-Iris-Distance, CASIA-Iris-Thousand, and CASIA-Iris-Syn are the three new subsets. A total of 54,607 iris photos from more than 1800 real participants and 1000 computer-

generated subjects are included in CASIA-IrisV4. All iris photos are 8-bit grey-level JPEG files that were either created artificially or acquired under near-infrared light.

#### 4.7.2. IIT Delhi Iris Database

The iris photographs taken from students and staff at IIT Delhi, New Delhi, India, make up the majority of the IIT Delhi Iris Database. This database was collected using a JIRIS, JPC1000, digital CMOS camera in the Biometrics Research Laboratory between January and July 2007 (work in progress). The database currently accessible contains images in bitmap format from 224 people. All of the subjects in the database are between the ages of 14 and 55, with 176 men and 48 girls. The 1120 images in the database are arranged into 224 folders, each with its own numerical identification or number. These photographs have a resolution of 320 by 240 pixels and were all taken in a controlled environment. We present a summary of IIT Delhi attribute in Table 4.

**Table 4.** A summary of IIT Delhi Iris Database attributes.

Attribute	Value
Number of images	1120
Number of people	224
Number of male	176
Number of female	48
Resolution	320 by 240 pixels

#### 4.8. Classification Metrics

There are four different kinds of records left over after the evaluation: true positives (TP), false positives (FP), true negatives (TN), and false negatives (FN). The metrics are then calculated as. Equations are used to calculate the categorization metrics (16–20) [43].

1. Predictive accuracy is defined as positive values and is given in Equation (12)

$$PPV = \frac{TP}{TP + FP} = 1 - FDR \quad (12)$$

where FDR stands for false discovery

2. Recall or sensitivity (true positive rate)

$$TPR = \frac{TP}{P} = \frac{TP}{TP + FN} = 1 - FNR \quad (13)$$

3. F-measure

$$F_1 = 2 \cdot \frac{\text{precision} \cdot \text{recall}}{\text{precision} + \text{recall}} = \frac{TP}{TP + \frac{1}{2}(FP + FN)} \quad (14)$$

4. G-mean

$$G - \text{mean} = \sqrt{\text{recall} \cdot \text{precision}} \quad (15)$$

5. Accuracy

$$ACC = \frac{TP + TN}{P + N} = \frac{TP + TN}{TP + TN + FP + FN} \quad (16)$$

Another way of calculating the accuracy is using this Equation (17)

$$acc = \frac{\text{number of true predictions}}{\text{total number prediction}} \quad (17)$$

We use the accuracy *acc* for reporting the performance of our algorithms in the evaluation.

## 5. Experimental Works and Evaluation

The evaluation is based on our recently developed VLBHO, comparing it with other meta-heuristic searching algorithms developed for feature selection in high dimensional space, namely, the algorithm developed in the work of [21]. For VLBHO, it has two ways for selecting the exemplar: it might use the position of stars for selecting the exemplar which is named position-based (P) or it might use the fitness of stars for selecting the exemplar which is named fitness based (F). Each of the two ways might be based on S or V shape transfer function from the continuous space to the binary space. Hence, we use the code presented in Table 5 for labelling the methods. We present a sample of the segmentation results before classification in Figure 3.

**Table 5.** Labelling code use for VLBHO.

Position Based, S Shape	Position Based, V Shape	Fitness Based, S Shape	Fitness Based, V Shape
PS	PV	FS	FV

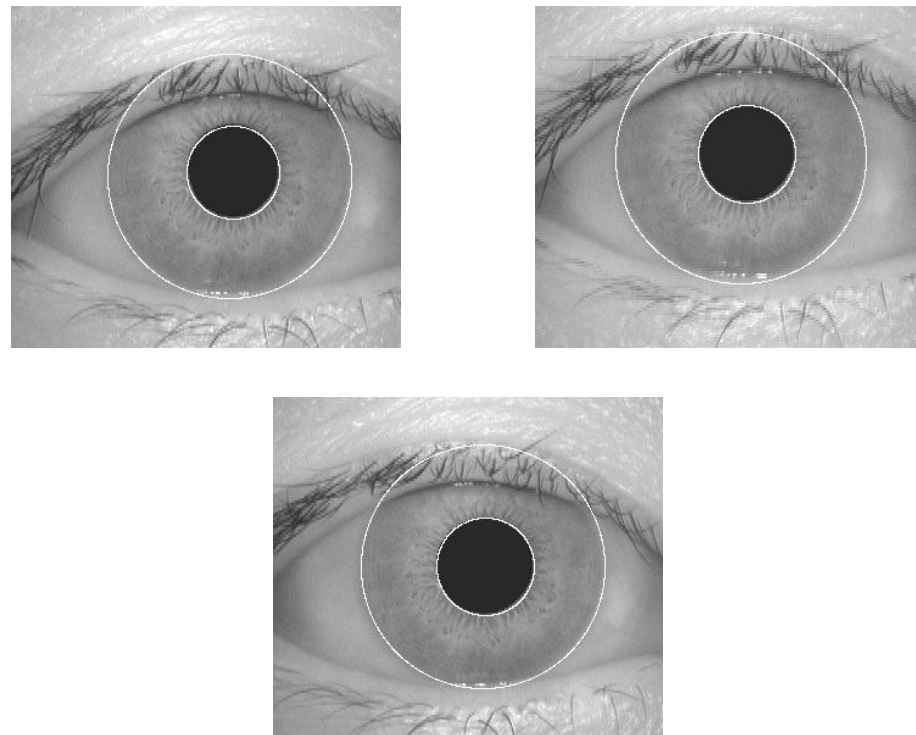


**Figure 3.** Samples of segmentation results.

For feature selection, we used two types of extractors LBP, and Gabor the parameters of each shown in Table 6.

**Table 6.** Datasets configuration of LBP and Gabor features extraction.

LBP		Gabor	
Parameter	Value	Value	Value
Radius	2	No. of scales	5
neighbors	8	No. of or entaions	8
Block size	16 16	filter bank s ze	size of image

We divide the feature space into segments based on the configuration provided in Table 7. The reason for using a segment size of 8 for Gabor compared with a segment size of 1 for LBP is the high number of features generated from Gabor so we used also principle component analysis (PCA) for projecting the features which reduced the features dimension by 95%. For classification, two models were used support vector machine (SVM) and logistic regression.

**Table 7.** Segment size for feature selection according to the type of feature.

Feature Name	Segment Size
Gabor	8
LBP	1

The performance metrics of our developed VLBHO are provided in Table 8. Observing the results, we find that PS and PV of VLBHO have outperformed other models. For Gabor features and SVM classifier, the best-achieved accuracy was 95.982% accomplished with PV. Similarly, PV was superior in terms of all other classification metrics. On the other side, for LBP features PS has accomplished the best classification results with 95.982% accuracy compared with only 80.804% accuracy for VLPSO.

**Table 8.** Classification metrics of our model compared with benchmarking VLPSO.

Feature Type	Classification Algorithm	Feature Selection Algorithm	Accuracy	F1 Score	Precision	Recall
Gabor	SVM	PS	0.93750	0.94107	0.94866	0.93750
		PV	<b>0.95982</b>	<b>0.96339</b>	<b>0.96875</b>	<b>0.95982</b>
		FS	0.94196	0.94628	0.95759	0.94196
		FV	0.93750	0.94286	0.95089	0.93750
		VLPSO	0.92857	0.93289	0.94420	0.92857
	LR	PS	0.99554	0.99583	0.99777	0.99554
		PV	0.99554	0.99583	0.99777	0.99554
		FS	0.99554	0.99583	0.99777	0.99554
		FV	0.99554	0.99583	0.99777	0.99554
		VLPSO	0.99554	0.99583	0.99777	0.99554
LBP	SVM	PS	<b>0.95982</b>	<b>0.95685</b>	<b>0.95848</b>	<b>0.95982</b>
		PV	0.92411	0.92217	0.93095	0.92411
		FS	0.92411	0.92381	0.93973	0.92411
		FV	0.91964	0.92054	0.93192	0.91964
		VLPSO	0.80804	0.80045	0.81920	0.80804
	LR	PS	<b>0.99107</b>	<b>0.99137</b>	0.99330	<b>0.99107</b>
		PV	0.95982	0.95714	<b>0.95848</b>	0.95982
		FS	0.98661	0.98869	0.99554	0.98661
		FV	0.94196	0.94449	0.95238	0.94196
		VLPSO	0.81696	0.81101	0.82813	0.81696

For summarization, we present the improvement percentage of VLBHO compared with VLPSO for Gabor and LBP. The results are shown in Table 9. As it is shown, VLBHO has achieved 21% improvement percentage over VLPSO for LBP features when it was called with PS mode which is the maximum improvement percentage.

**Table 9.** Improvement percentage of VLBHO over VLPSO with respect to Gabor features and LBP and different classifiers.

Feature Type	Classification Algorithm	Feature Selection Algorithm	Accuracy	IP
Gabor	SVM	VLBHO-PS VLPSO	<b>0.95982</b> 0.92857	3%
	LR	VLBHO-FV VLOPSO	0.99554 0.99554	0%
LBP	SVM	VLBHO-PS VLPSO	<b>0.95982</b> 0.80804	18%
	LR	VLBHO-PS VLOPSO	<b>0.99107</b> 0.81696	21%

## 6. Summary and Conclusions

In this article, feature encoding and selection for iris recognition have been presented. Adopting our current algorithm variable length black hole optimization enables selecting variable length features for iris identification (VLBHO). Our proposed technique allows for segment-based feature decomposition based on relevance, making the optimization more efficient in terms of memory and computation, as well as more promising in terms of convergence. The article uses SVM and logistics for classification. The approach has been evaluated based on two iris benchmarking datasets and compared with various models in the literature. It has shown the superiority of our recognition that uses variable length black hole optimization for feature encoding and selection. The results provide reduced feature space with high accuracy. Some limitations can be addressed such as the sensitivity to the initial population. Such limitation can be solved by incorporating heuristic population initialization. Future work is to compare with other models for feature selection with variable length functionality.

**Author Contributions:** Conceptualization, T.O.Q.S., N.F. and N.S.A.M.T.; Formal analysis, T.O.Q.S., N.F. and N.S.A.M.T.; Visualization, T.O.Q.S. and N.F.; Writing—review & editing, N.S.A.M.T. All authors have read and agreed to the published version of the manuscript.

**Funding:** This research received no external funding.

**Institutional Review Board Statement:** Not applicable.

**Informed Consent Statement:** Not applicable.

**Data Availability Statement:** All data were presented in the main text.

**Conflicts of Interest:** The authors declare no conflict of interest.

## References

1. Malarvizhi, N.; Selvarani, P.; Raj, P. Adaptive fuzzy genetic algorithm for multi biometric authentication. *Multimed. Tools Appl.* **2020**, *79*, 9131–9144. [[CrossRef](#)]
2. Duarte, T.; Pimentão, J.P.; Sousa, P.; Onofre, S. Biometric access control systems: A review on technologies to improve their efficiency. In Proceedings of the 2016 IEEE International Power Electronics and Motion Control Conference (PEMC), Varna, Bulgaria, 25–28 September 2016; pp. 795–800.
3. Labati, R.D.; Genovese, A.; Muñoz, E.; Piuri, V.; Scotti, F.; Sforza, G. Biometric recognition in automated border control: A survey. *ACM Comput. Surv.* **2016**, *49*, 1–39. [[CrossRef](#)]
4. Goode, A. Biometrics for banking: Best practices and barriers to adoption. *Biom. Technol. Today* **2018**, *2018*, 5–7. [[CrossRef](#)]
5. Rajput, P.; Mahajan, K. Dental biometric in human forensic identification. In Proceedings of the 2016 International Conference on Global Trends in Signal Processing, Information Computing and Communication (ICGTSPICC), Jalgaon, India, 22–24 December 2016; pp. 409–413.
6. Linsangan, N.B.; Panganiban, A.G.; Flores, P.R.; Poligratis, H.A.T.; Victa, A.S.; Torres, J.L.; Villaverde, J. Real-time Iris Recognition System for Non-Ideal Iris Images. In Proceedings of the 2019 11th International Conference on Computer and Automation Engineering, Perth, Australia, 23–25 February 2019; pp. 32–36.

7. Indrawal, D.; Waykole, S.; Sharma, A. Development of Efficient and Secured Face Recognition using Biometrics. *Int. J. Electron. Commun. Comput. Eng.* **2019**, *10*, 183–189.
8. Jain, A.K.; Prabhakar, S.; Pankanti, S. On the similarity of identical twin fingerprints. *Pattern Recognit.* **2002**, *35*, 2653–2663. [[CrossRef](#)]
9. Raut, S.D.; Humbe, V.T. Biometric palm prints feature matching for person identification. *Int. J. Mod. Educ. Comput. Sci.* **2012**, *4*, 61. [[CrossRef](#)]
10. Al-Kateeb, Z.N.; Mohammed, S.J. Encrypting an audio file based on integer wavelet transform and hand geometry. *TELKOMNIKA Indones. J. Electr. Eng.* **2020**, *18*, 2012–2017. [[CrossRef](#)]
11. Seong, J.-w.; Lee, H.-j.; Cho, S.-h. A Study on the Voice Security System Using Sensor Technology. In Proceedings of the 2020 IEEE International Conference on Big Data and Smart Computing (BigComp), Busan, Korea, 19–22 February 2020; pp. 520–525.
12. Pathan, M.; Singh, G.; Yelane, A. Vein Pattern Recognition and Authentication Based on Gradient Feature Algorithm. Available online: <http://shabdbooks.com/gallery/spl-175.pdf> (accessed on 1 June 2022).
13. Huo, G.; Guo, H.; Zhang, Y.; Zhang, Q.; Li, W.; Li, B. An effective feature descriptor with Gabor filter and uniform local binary pattern transcoding for Iris recognition. *Pattern Recognit. Image Anal.* **2019**, *29*, 688–694. [[CrossRef](#)]
14. Daugman, J. Statistical richness of visual phase information: Update on recognizing persons by iris patterns. *Int. J. Comput. Vis.* **2001**, *45*, 25–38. [[CrossRef](#)]
15. Quinn, G.W.; Quinn, G.W.; Grother, P.; Matey, J. *IREX IX Part One: Performance of Iris Recognition Algorithms*; US Department of Commerce, National Institute of Standards and Technology: Gaithersburg, MD, USA, 2018.
16. Kaur, B.; Singh, S.; Kumar, J. Robust iris recognition using moment invariants. *Wirel. Pers. Commun.* **2018**, *99*, 799–828. [[CrossRef](#)]
17. Hancer, E.; Xue, B.; Zhang, M. Differential evolution for filter feature selection based on information theory and feature ranking. *Knowl.-Based Syst.* **2018**, *140*, 103–119. [[CrossRef](#)]
18. Daugman, J. Information theory and the iriscodes. *IEEE Trans. Inf. Forensics Secur.* **2015**, *11*, 400–409. [[CrossRef](#)]
19. Crawford, B.; Soto, R.; Astorga, G.; García, J.; Castro, C.; Paredes, F. Putting continuous metaheuristics to work in binary search spaces. *Complexity* **2017**, *2017*, 8404231. [[CrossRef](#)]
20. Rodríguez-Molina, A.; Mezura-Montes, E.; Villarreal-Cervantes, M.G.; Aldape-Pérez, M. Multi-objective meta-heuristic optimization in intelligent control: A survey on the controller tuning problem. *Appl. Soft Comput.* **2020**, *93*, 106342. [[CrossRef](#)]
21. Tran, B.; Xue, B.; Zhang, M. Variable-length particle swarm optimization for feature selection on high-dimensional classification. *IEEE Trans. Evol. Comput.* **2018**, *23*, 473–487. [[CrossRef](#)]
22. Wong, W.; Ming, C.I. A review on metaheuristic algorithms: Recent trends, benchmarking and applications. In Proceedings of the 2019 7th International Conference on Smart Computing & Communications (ICSCC), Sarawak, Malaysia, 28–30 June 2019; pp. 1–5.
23. Zhang, B.; Gao, Y.; Zhao, S.; Liu, J.Z. Local Derivative Pattern Versus Local Binary Pattern: Face Recognition with High-Order Local Pattern Descriptor. *IEEE Trans. Image Process.* **2009**, *19*, 533–544. Available online: <https://ieeexplore.ieee.org/document/5308376/> (accessed on 1 June 2022). [[CrossRef](#)]
24. Hu, Y.; Sirlantzis, K.; Howells, G.; Security. Optimal generation of iris codes for iris recognition. *IEEE Trans. Inf. Forensics* **2016**, *12*, 157–171. [[CrossRef](#)]
25. He, F.; Han, Y.; Wang, H.; Ji, J.; Liu, Y.; Ma, Z. Deep learning architecture for iris recognition based on optimal Gabor filters and deep belief network. *J. Electron. Imaging* **2017**, *26*, 023005. [[CrossRef](#)]
26. Lim, S.; Lee, K.; Byeon, O.; Kim, T. Efficient iris recognition through improvement of feature vector and classifier. *ETRI J.* **2001**, *23*, 61–70. [[CrossRef](#)]
27. Daugman, J. High Conf Visual Recog of Persons by a test of statistical significance. *IEEE Trans. Pattern Anal. Mach. Intell* **1993**, *15*, 1148–1161. [[CrossRef](#)]
28. Boles, W.; Boashash, B. Iris Recognition for Biometric Identification using dyadic wavelet transform zero-crossing. *IEEE Trans. Signal Process.* **1998**, *46*, 1185–1188. [[CrossRef](#)]
29. Adamović, S.; Mišković, V.; Maček, N.; Milosavljević, M.; Šarac, M.; Saračević, M.; Gnjatović, M. An efficient novel approach for iris recognition based on stylometric features and machine learning techniques. *Future Gener. Comput. Syst.* **2020**, *107*, 144–157. [[CrossRef](#)]
30. Xiao, L.; Sun, Z.; He, R.; Tan, T. Coupled feature selection for cross-sensor iris recognition. In Proceedings of the 2013 IEEE Sixth International Conference on Biometrics: Theory, Applications and Systems (BTAS), Arlington, VA, USA, 29 September–2 October 2013; pp. 1–6.
31. Garg, M.; Arora, A.; Gupta, S. An Efficient Human Identification Through Iris Recognition System. *J. Signal Process. Syst.* **2021**, *93*, 701–708. [[CrossRef](#)]
32. Raghavendra, C.; Kumaravel, A.; Sivasuramanyan, S. Features subset selection using improved teaching learning based optimisation (ITLBO) algorithms for IRIS recognition. *Indian J. Sci. Technol.* **2017**, *10*, 1–12. [[CrossRef](#)]
33. Ma, J.; Gao, X. A filter-based feature construction and feature selection approach for classification using Genetic Programming. *Knowl.-Based Syst.* **2020**, *196*, 105806. [[CrossRef](#)]
34. Vatsa, M.; Singh, R.; Noore, A. Improving iris recognition performance using segmentation, quality enhancement, match score fusion, and indexing. *IEEE Trans. Syst. Man Cybern. Part B* **2008**, *38*, 1021–1035. [[CrossRef](#)]

35. Choudhary, M.; Tiwari, V.; Venkanna, U. An approach for iris contact lens detection and classification using ensemble of customized DenseNet and SVM. *Future Gener. Comput. Syst.* **2019**, *101*, 1259–1270. [[CrossRef](#)]
36. Raghavendra, R.; Raja, K.B.; Busch, C. Contlensnet: Robust iris contact lens detection using deep convolutional neural networks. In Proceedings of the 2017 IEEE Winter Conference on Applications of Computer Vision (WACV), Santa Rosa, CA, USA, 24–31 March 2017; pp. 1160–1167.
37. Zhang, H.; Sun, Z.; Tan, T. Contact lens detection based on weighted LBP. In Proceedings of the 2010 20th International Conference on Pattern Recognition, Istanbul, Turkey, 23–26 August 2010; pp. 4279–4282.
38. Yadav, D.; Kohli, N.; Doyle, J.S.; Singh, R.; Vatsa, M.; Bowyer, K.W. Unraveling the effect of textured contact lenses on iris recognition. *IEEE Trans. Inf. Forensics Secur.* **2014**, *9*, 851–862. [[CrossRef](#)]
39. Chen, Y.; Wu, C.; Wang, Y. T-center: A novel feature extraction approach towards large-scale iris recognition. *IEEE Access* **2020**, *8*, 32365–32375. [[CrossRef](#)]
40. Bastys, A.; Kranauskas, J.; Masiulis, R. Iris recognition by local extremum points of multiscale Taylor expansion. *Pattern Recognit.* **2009**, *42*, 1869–1877. [[CrossRef](#)]
41. Cheng, Y.; Liu, Y.; Zhu, X.; Li, S. A multiclassification method for iris data based on the hadamard error correction output code and a convolutional network. *IEEE Access* **2019**, *7*, 145235–145245. [[CrossRef](#)]
42. Hatamlou, A. Black hole: A new heuristic optimization approach for data clustering. *Inf. Sci.* **2013**, *222*, 175–184. [[CrossRef](#)]
43. Hameed, I.M.; Abdulhussain, S.H.; Mahmmod, B.M. Content-based image retrieval: A review of recent trends. *Cogent Eng.* **2021**, *8*, 1927469. [[CrossRef](#)]